Supporting information

Structural and Spectroscopic Characterization of Pyrene Derived Carbon Nano Dots: A Single-Particle Level Analysis

*Gayatri Batra,[1, 2, ¥]¶ Shubham Sharma, [1, 2]¶ Kush Kaushik, [1, 2] Chethana Rao, [1, 2] Pawan Kumar, [3,4] Krishan Kumar, [1, 2] Subrata Ghosh, [1, 2] Deep Jariwala, [3] Eric A. Stach,[4] Aditya Yadav[1, 2] * and Chayan Kanti Nandi[1, 2]*

[1]School of Basic Sciences, Indian Institute of Technology, Mandi, HP-175001, India.

[2]Advanced Materials Research Centre, Indian Institute of Technology, Mandi, HP-175001, India.

[3]Department of Electrical and Systems Engineering, University of Pennsylvania, Philadelphia, PA-19104

[4]Department of Materials Science and Engineering, University of Pennsylvania, Philadelphia, PA-19104

Current address
[¥]Deutsches Elektronrn-Synchrotron (DESY), Notkestraße 85, 22607, Hamburg, Germany

¶ *Gayatri Batra and Shubham Sharma have contributed equally to the work*

1. Experimental

Materials:

All glassware was washed with aqua regia, followed by rinsing several times with double-distilled water. Pyrene was purchased from Alfa Aesar. HCl and HNO_3 were purchased from fisher scientific. All chemicals were used without further purification. Double-distilled (18.3 mΩ) deionized water (ELGA PURELAB Ultra) was used throughout the entire process.

2. Characterization

The UV-Vis absorption spectra were recorded using Shimadzu UV-Vis 2450 spectrophotometer. The spectra were collected using a quartz cuvette having a 10 mm path length and 1 ml volume. Steady-state fluorescence spectra were recorded on a Horiba spectrophotometer. The fluorescence lifetime was measured using Horiba Scientific Delta Flex TCSPC system with a pulsed LED source (454 nm). All measurements were performed in water. Ludox has been used to calculate IRF for de-convolution of the spectral value. Powder X-ray diffraction (PXRD) pattern was recorded on a Rigaku Smart Lab diffractometer, using Cu-K_α radiation from 5° to 80° with a scanning rate of 2°/min. The particles' shape and structure were analyzed by transmission electron microscopy (TEM) using FEI Tecnai equipped with a

LaB6 source and JEOL (F-200) containing cold-field emission gun, microscopes operating at 200 kV. An aberration-corrected (probe correction) JEOL NEOARM microscope, used for scanning transmission electron microscopy (STEM) operated at an accelerating voltage of 200 kV. High-angle annular dark-field (HAADF) STEM images were acquired with 1Å probe diameter at a convergence angle of 25–29 mrad and the condenser lens aperture was kept at 40 μm with a camera length of 4 cm, probe current measured was 120 pAmp. The captured STEM images were collected using GATAN GMS (v3) application and associated GATAN dark-field high-angle annular detector. The Raman spectrum was measured by the confocal microscope Raman spectrometer (Horiba Scientific, XploRA ONE). A 532 nm laser was used to excite the sample. Thermal properties were measured by Perkin Elmer Pyris Thermogravimetric (TGA) analyzer under a nitrogen atmosphere with a heating rate of 10 °C min^{-1}. A field emission scanning electron microscopy FESEM (NOVA NanoSEM 450) at an accelerating voltage of 10 kV was used to capture SEM images. Fourier transforms infrared (FTIR) spectra were measured using a Perkin-Elmer FTIR spectrophotometer equipped with a horizontal attenuated total reflectance (ATR) accessory containing a zinc selenide crystal and operating at 4 cm^{-1} resolution. The use of spectral subtraction provided reliably reproducible results. HRMS spectra were recorded on a Bruker impact-HD spectrometer and ^{1}H NMR spectra were recorded on a Jeol-ECX-500 MHz spectrometer using tetramethylsilane (TMS) as an internal standard. X-ray photoelectron spectroscopy (XPS) measurements were carried out on a NEXSA surface analysis model by Thermo Fisher Scientific using Al-K_α (1486.6 eV) X-ray radiation. The XPS data were acquired with a spot size 400 μm having a standard lens mode.

3. Synthesis procedures for CNDs using top-down approach

Synthesis of Graphene Oxide from Graphite (Hummer's Method):

Graphite (2.0 g) was dissolved in 27 mL of H_2SO_4 and sodium nitrate (0.5 g). The mixture was then stirred at room temperature for 1 h and $KMnO_4$ (3 g) was added using ice bath and the mixture was stirred at 40 °C for 12 h and Distilled water (500 mL) was added and stirring was done for 1.5 h and hydrogen peroxide (5 mL) was added and the reaction mixture was left undisturbed, and decantation was done, and the as prepared Graphene oxide was washed with DI and HCl and dried.

Synthesis of CNDs from GO using NaOH:

Graphene Oxide (0.2 g) was dissolved in 5 M NaOH (20 mL) and the mixture was then sonicated for 5 minutes and then transferred to a hydrothermal autoclave reactor (50 mL) and heated at 180°C for 12 h. The reactor was cooled to room temperature and the reaction mixture was filtered with a 0.22 µm polyvinylidene difluoride microporous membrane to remove unreacted part of GO and dialysis was done to remove salt ions.

4. Absolute quantum yield measurements using integration sphere method

The quantum yield (Φ_F) of fluorescence is defined as the ratio of the number of emitted photons and the number of absorbed photons during the excitation of a sample under investigation.

$$Quantum\ Yield\ = \frac{Total\ emitted\ photon}{Total\ absorbed\ photon}$$

These are the spectra we can record using flourolog during absolute quantum yield.

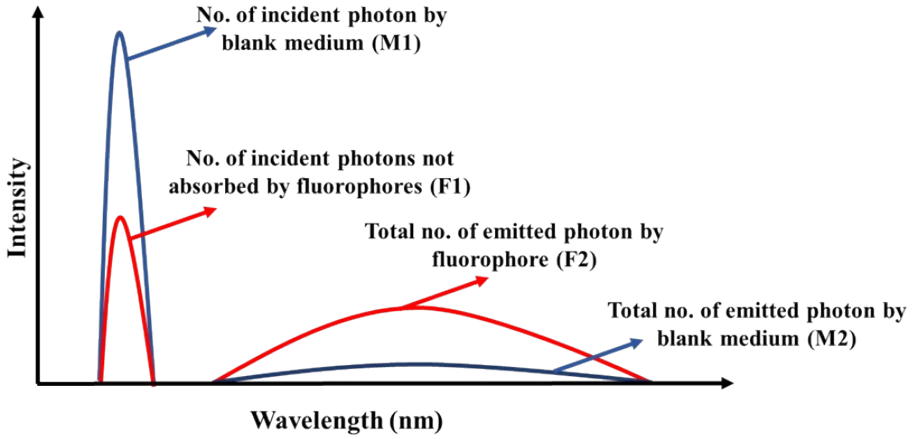

$$Absolute\ Quantum\ Yield = \frac{Total\ emitted\ photon\ (F2 - M2)}{Total\ absorbed\ photon\ (\ M1 - F1)}$$

Total emitted photon = Area under F2 region - Area under M2 region

Total absorbed photon = Area under M1 region - Area under F1 region

5. Single-molecule time trace and photon counts

All the separated components were spin-coated on a cleaned glass coverslip to collect single-molecule time traces. The diffraction-limited spots produced due to single-molecule blinking were observed using the 100x Nikon TIRF objective. A 488 nm diode laser with 40 mW maximum power was used. An oil immersion Nikon TIRF objective (100x magnification and 1.49 NA) was mounted on a custom build inverted optical microscope (Nikon Ti

epifluorescence microscope). A 488 nm high pass Dichroic (AHF Analysentechnik) was used to separate the excitation and emission light, and a bandpass filter of 575/50 is used to further reject the excitation laser and allow the emission of the fluorophores. Andor EMCCD iXon Ultra 897 was used to record the single-molecule photon events at the frame rate of 17 MHz and exposure time of 50 ms, and EM gain of 300. The single-particle movie is made on a 128x128 pixel area which corresponds to the 20.48 µm x 20.48 µm area, and a single-pixel corresponds to the 160 nm x 160 nm area. A fluorophore creates a diffraction-limited spot of ~ 3x3 pixels, and each of these spots was analyzed as a single-particle and is further used for the photon count analysis. The time trajectories were recorded and analyzed using the Andor Solis 32 bit software. The incident photons were converted to electrons and subsequent to digital counts by the EMCCD. The Andor Solis and Matlab were used to extract the total photon counts. The movies recorded under the kinetic mode of EMCCD, time/frame trajectories of the counts/intensity at a given pixel, were obtained for the provided exposure time. These time trajectories were saved for further analysis.

6. **Confocal imaging of cells labelled with three separated components**

Coverslip preparation: The glass slides and coverslips were cleaned by incubating in freshly prepared Piranha solution for 30 min and finally washing by MiliQ water in bath sonication then dried under nitrogen.

Cell culture, fixation and staining: HeLa cells were grown in Dulbecco's Modified Eagle Medium (DMEM) with 10% fetal bovine serum. The cells were grown in 6-well plate on the coverslips with a density of 10^4 cells per 100 µl. Each well was filled with 2 ml of cell suspension in growth medium and the cells were allowed to grow overnight for proper adherence and growth. The growth and the attachment of the cells to the coverslips were examined by an optical microscope. Once the cells reached proper confluency, they were fixed by incubating with 4% paraformaldehyde solution in 1x PBS buffer for 5 min. After fixation, the cells were permeabilized by 10 min incubation in 0.1% triton. The fixed and permeabilized cells were washed 4-6 times by PBS buffer to remove extra agents. These cells were incubated with the bright green, greenish brown and deep brown components at room temperature to achieve enough labelling density for confocal. The coverslips were fixed on a glass slide before imaging.

Confocal microscopy: Nikon Eclipse Ti inverted microscope was used for the confocal microscopy and images were acquired using Nikon Nis-Element software. The cell samples

were excited by the three lasers 488, 561 and 639 nm. Finally, the images were collected by choosing a proper filter set.

7. Characterization of Pyrene

FTIR: FTIR spectrum shows the characteristic vibration at 3043 cm^{-1} for C-H stretching mode, 1592 cm^{-1} for C=C stretching, 1181 cm^{-1} for C=C bending, 832, 702 cm^{-1} for C-H bending.

^{1}H NMR (500 MHz, $CDCl_3$): δ 8.14 (d, J = 7.55 Hz, 4H), 8.04 (s, 4H), 7.97 (t, J_1 = 7.6 Hz, J_2 = 7.55 Hz, 2H).

HRMS: The actual calculated *m/z* for pyrene ($C_{10}H_{16}$) is 202. The mass spectra given in figure, shows the peak with *m/z* = 202.

8. Characterization of 1,3,6 trinitropyrene (TNP):

After the synthesis of 1,3,6-trinitropyrene (TNP), first, we characterized the TNP using ^{1}H-NMR, HRMS and FTIR.

FTIR: FTIR spectrum shows the characteristic vibration at 3080 cm^{-1} for C-H stretching mode, 1580 cm^{-1} for C=C vibration, 1518 cm^{-1} for NO_2 asymmetric mode, 1348 cm^{-1} for NO_2 symmetric mode and 845 for C-H vibration.

^{1}H NMR (500 MHz, DMSO-d6): δ 9.41 (s, 1H), 9.23 (d, J = 10.3 Hz, 1H), 9.16 (d, J = 9.6 Hz, 1H), 9.08 (d, J = 9.6 Hz, 1H), 8.86 (d, J = 8.25 Hz, 1H), 8.59 (d, J = 8.9 Hz, 2H).

HRMS: The actual calculated *m/z* for $C_{16}H_7N_3O_6$ (TNP) is 337. The mass spectra given in figure, shows peak at *m/z* = 337 and the adduct ion peak with *m/z* = 338 $(C_{16}H_7N_3O_6 + H)^+$. Strong adduct ion peak with *m/z* = 360 $(C_{16}H_7N_3O_6 + Na)^+$.

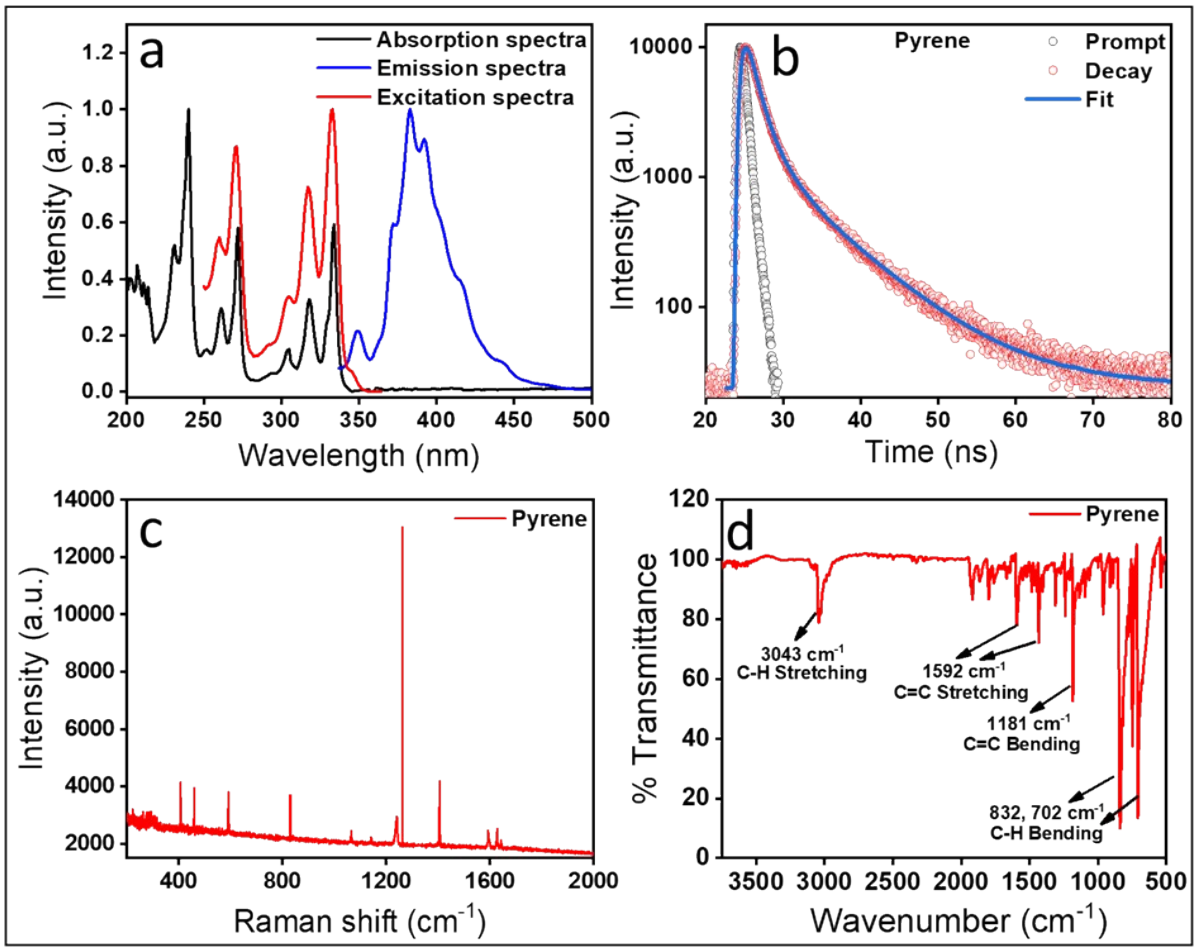

Fig. S1 (a) Absorption, emission and excitation spectra of pyrene. (b) Lifetime of pyrene with an average lifetime of 1.65 ns. (c) Raman and (d) FTIR spectra of pyrene with the characteristics vibrational modes.

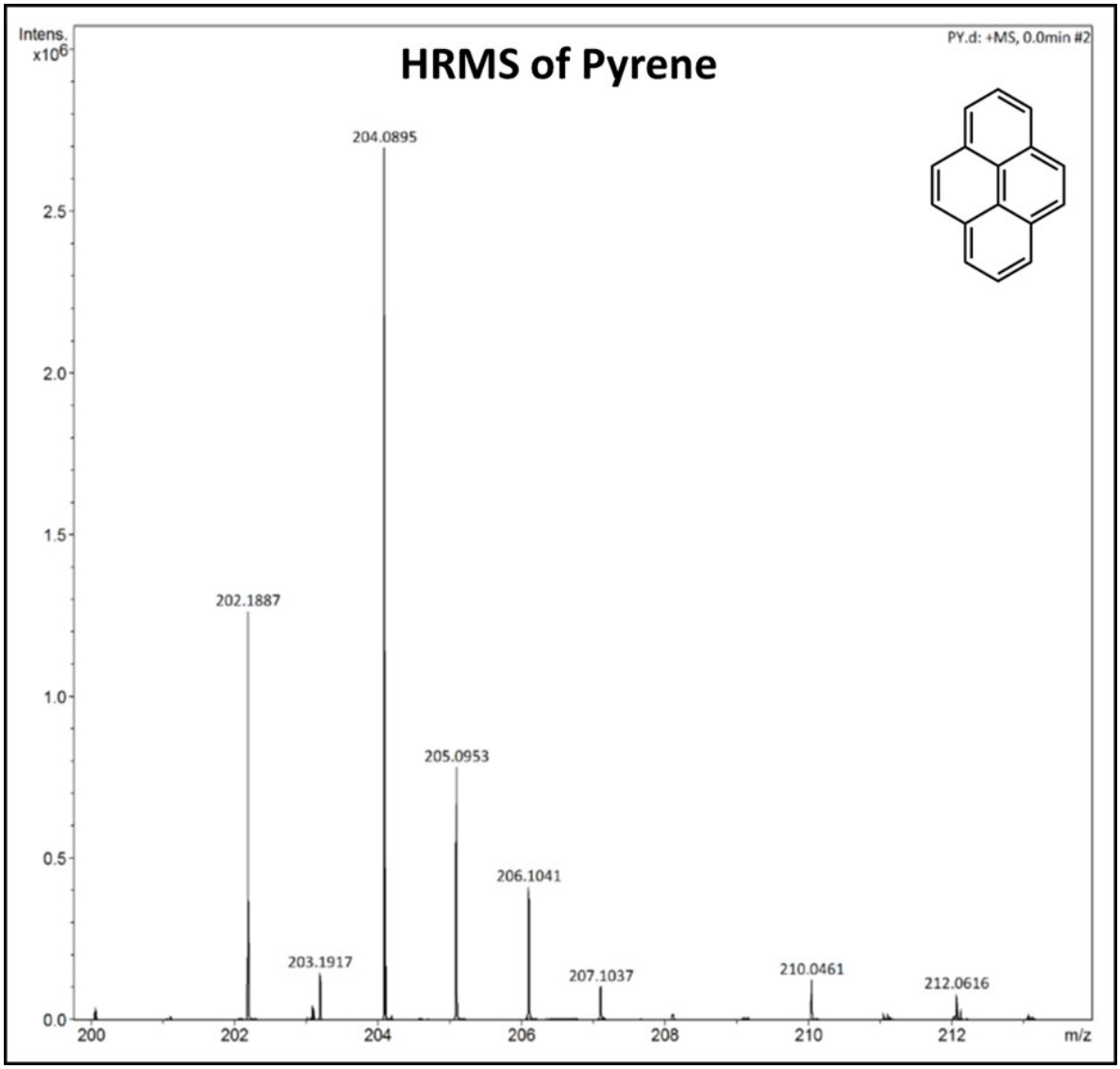

Fig. S2 HRMS spectra of pyrene.

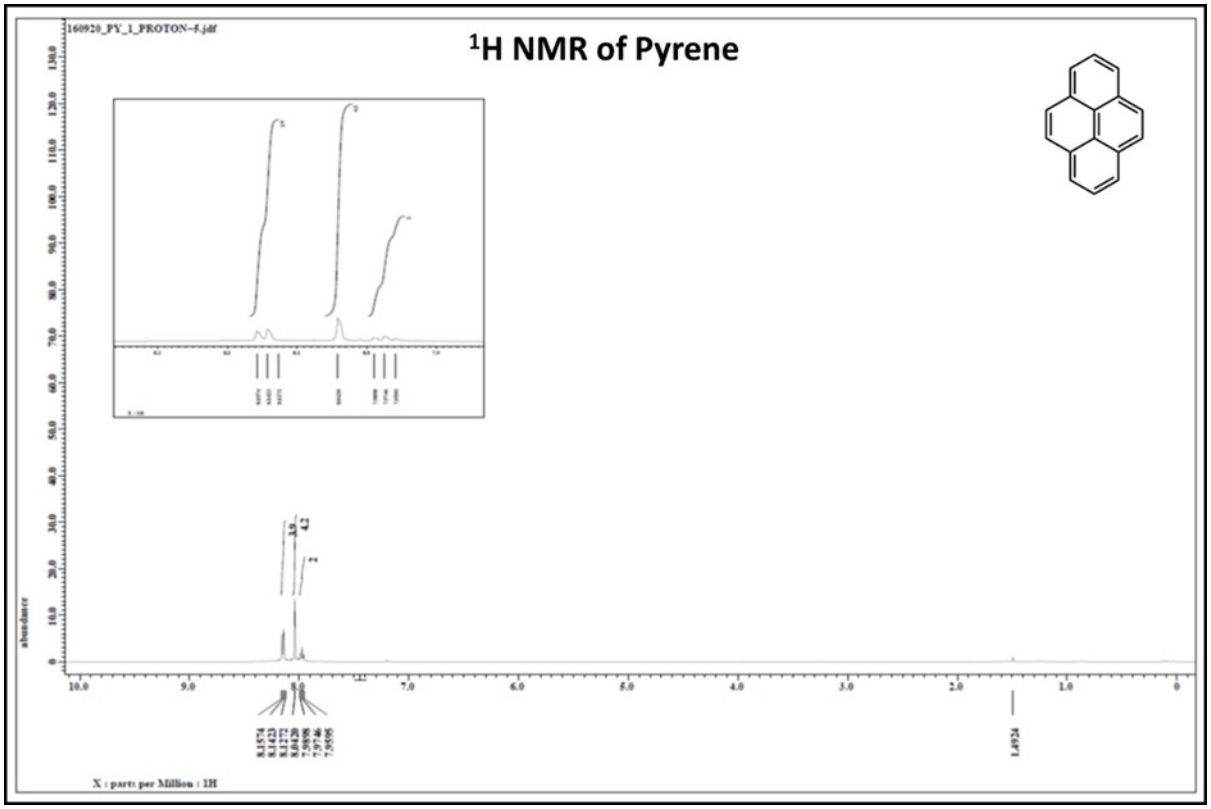

Fig. S3 ^{1}H NMR spectra of pyrene.

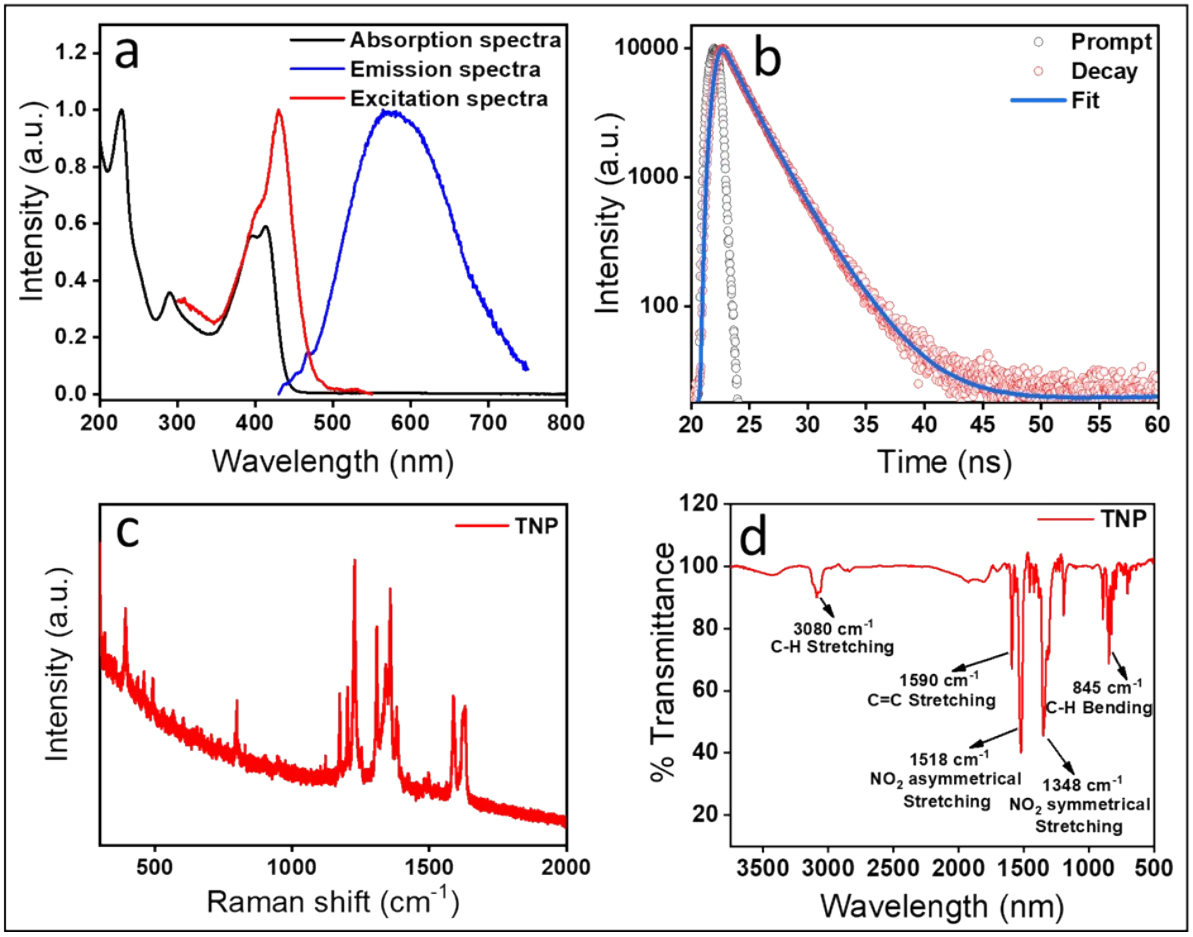

Fig. S4 (a) Absorption, emission and excitation spectra of TNP. (b) Lifetime of TNP with an average lifetime of 2.43 ns. (c) Raman spectra and (d) FTIR spectrum of TNP with the characteristics vibrational modes.

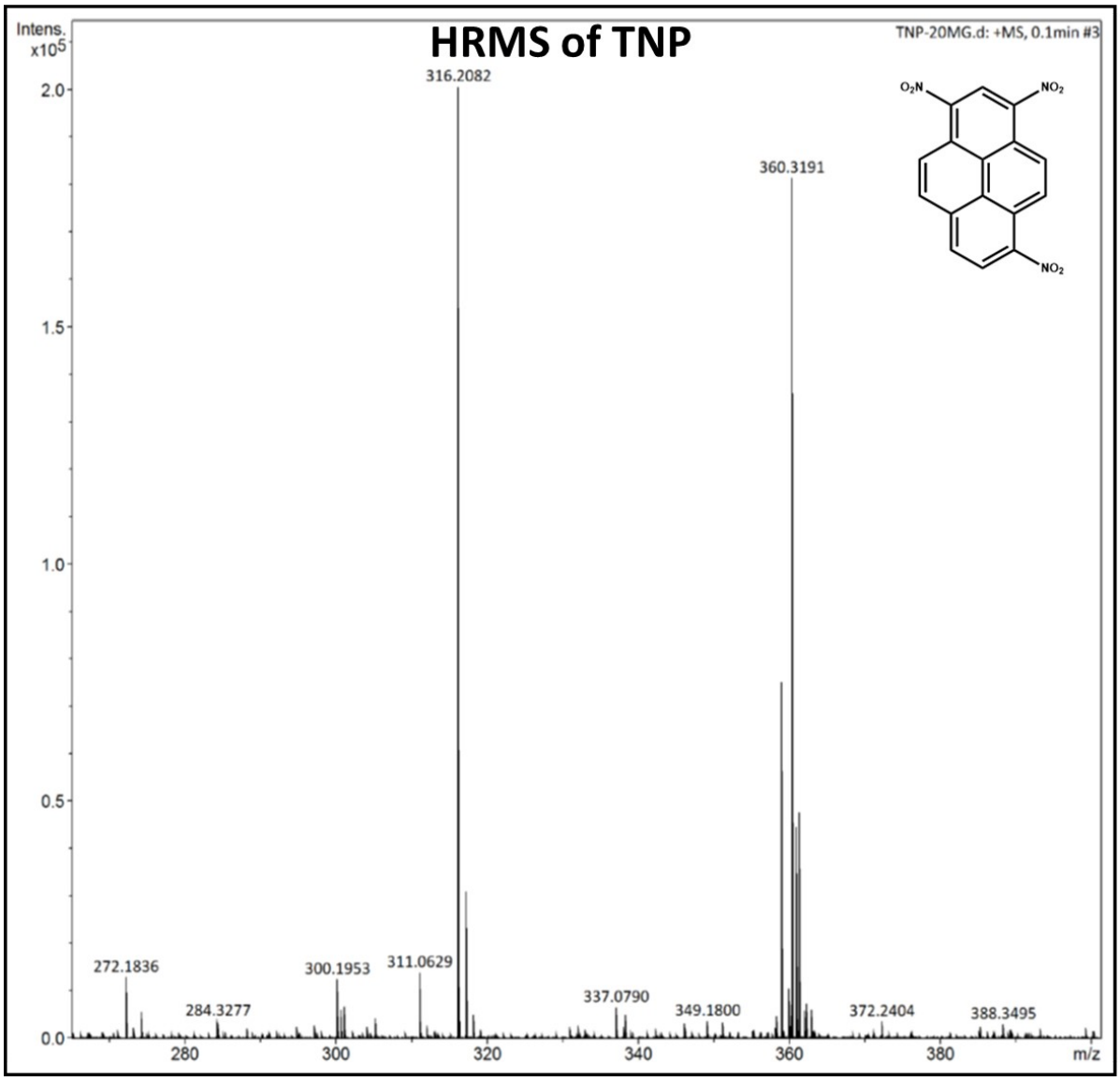

Fig. S5 HRMS spectra of TNP.

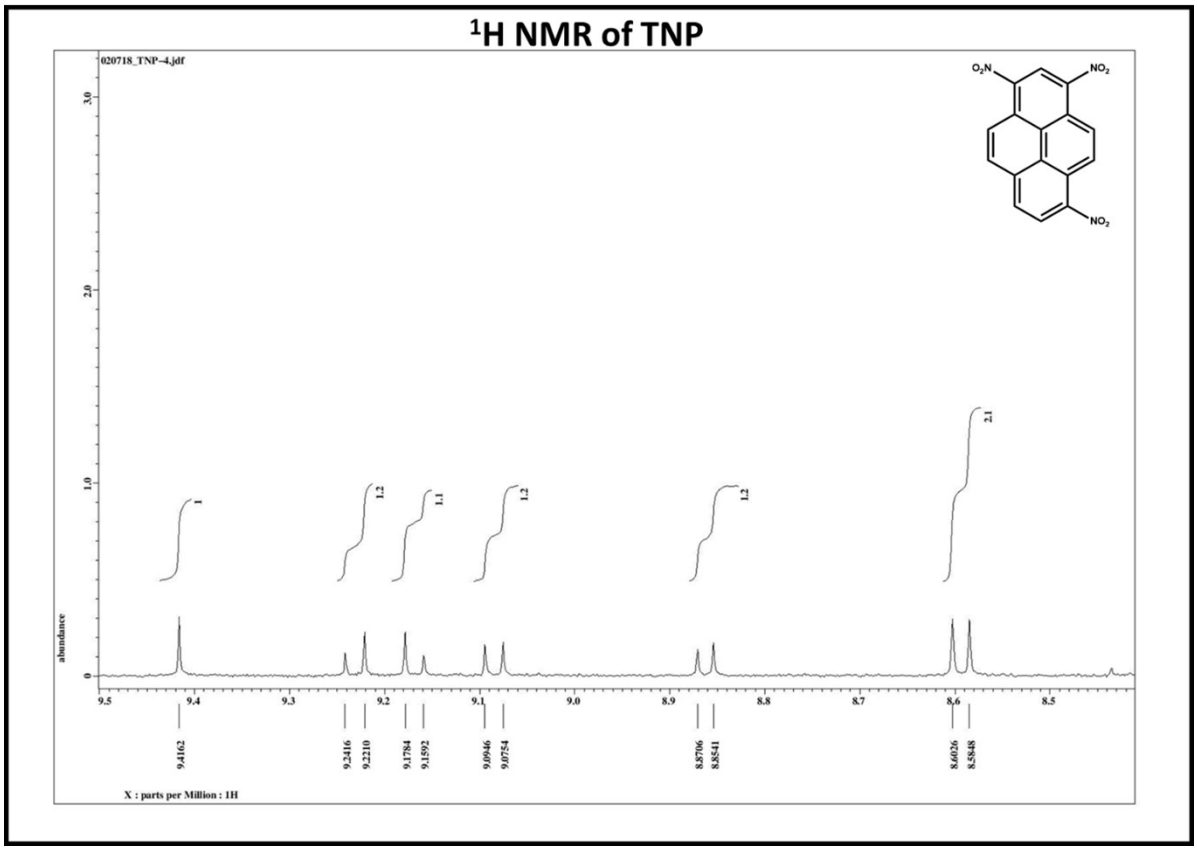

Fig. S6 ^{1}H NMR spectra of TNP.

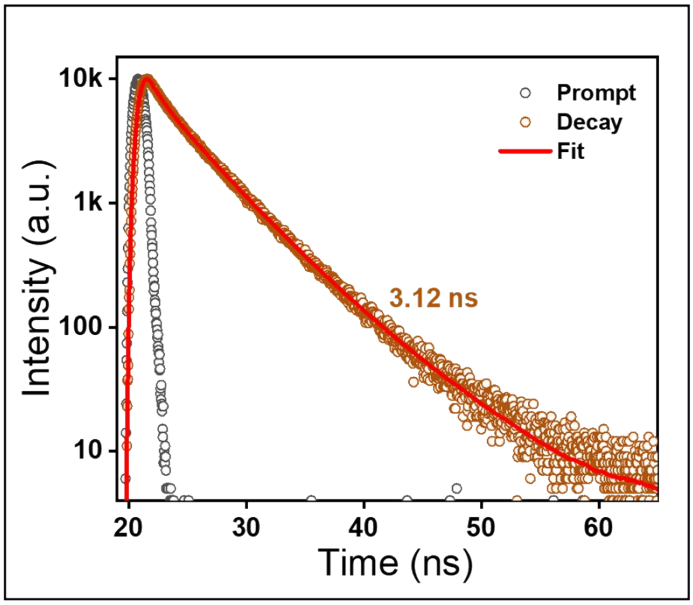

Fig. S7 Lifetime decay of crude CNDs with an average lifetime of 3.12 ns.

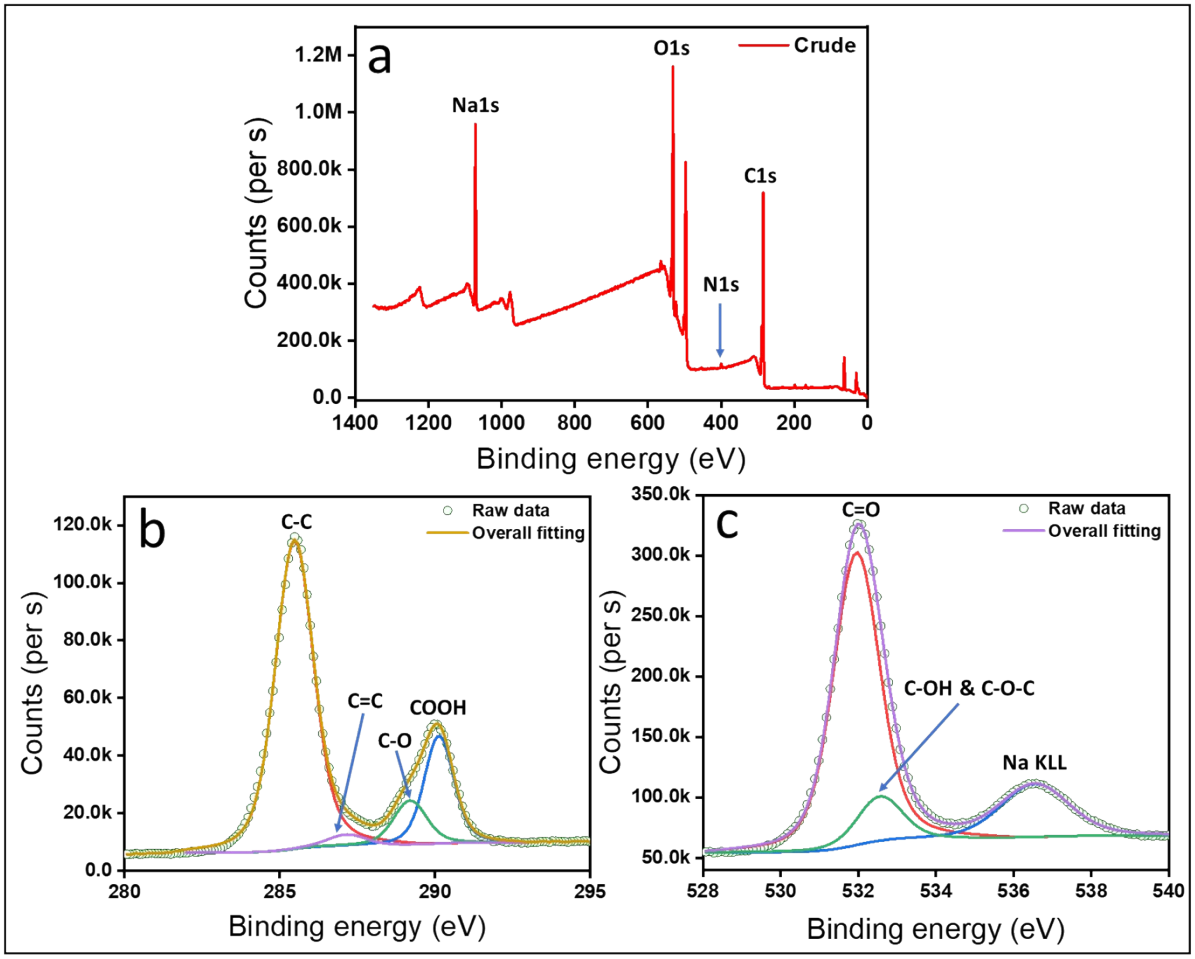

Fig. S8 (a) XPS spectra of crude CNDs. (b-c) High-resolution XPS spectra of C1s where peaks at 285.49, 287.18, 289.22 and 290 eV representing the C-C, C=C, C-O and COOH functional groups respectively. (c) High-resolution XPS spectra of O1s where peaks at 531.93 and 532.58 eV representing the C=O, C-OH & C-O-C functional groups.

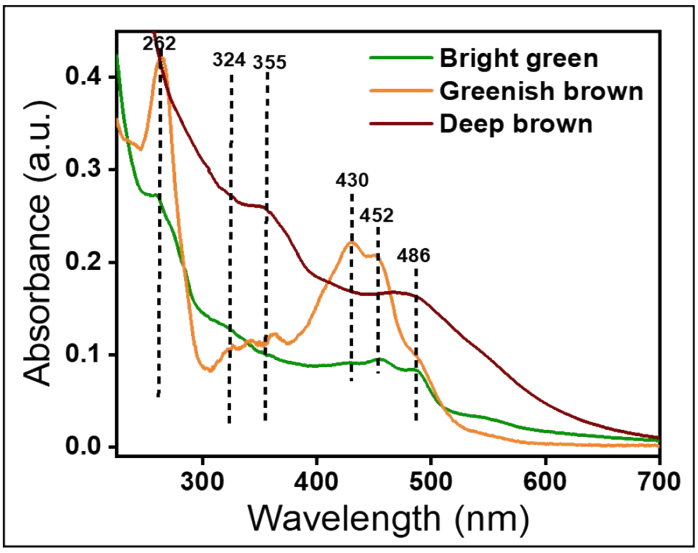

Fig. S9 Zoomed absorption spectra of purified component.

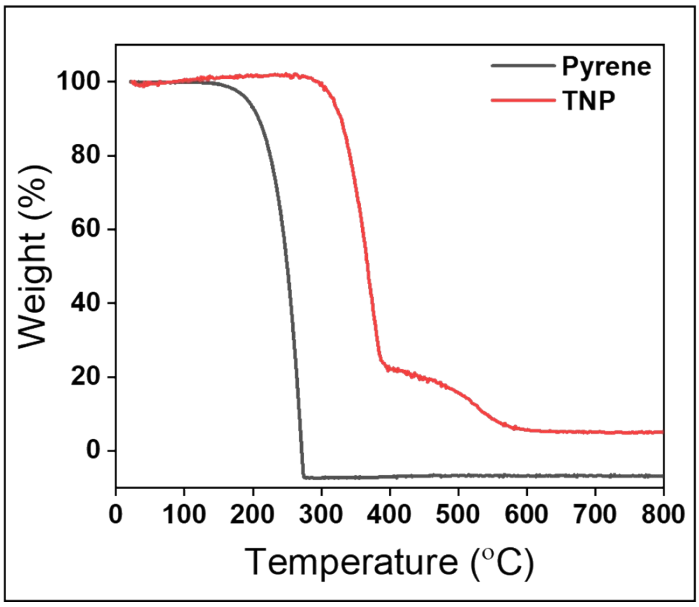

Fig. S10 Comparative TGA spectra of pyrene and TNP. A complete mass loss for pyrene was observed within 280 °C, while TNP showed 80% mass loss within 400 °C.

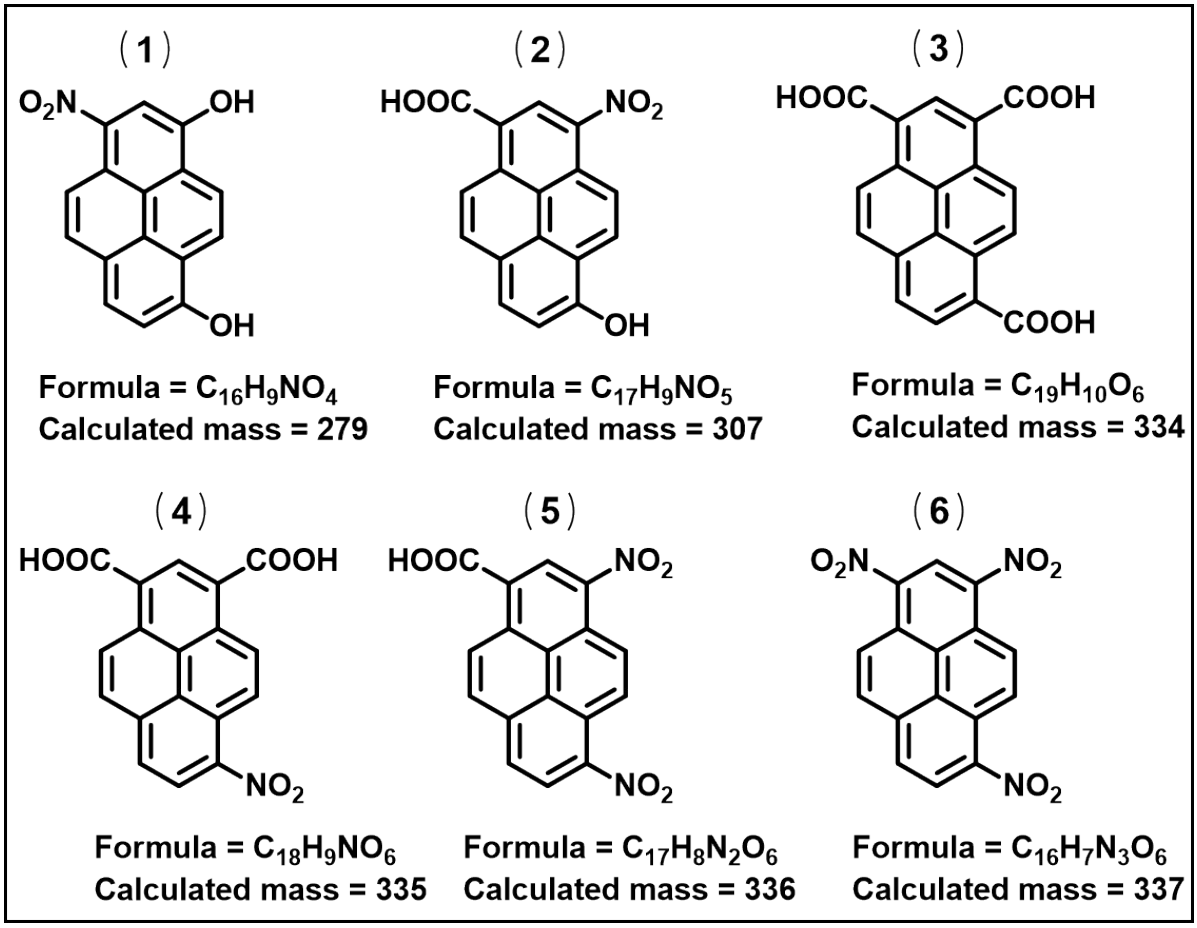

Fig. S11 Possible structures of molecular fluorophores containing -OH/-COOH/-NO_2 functional groups and their calculated mass (predicted based on XPS, FT-IR and mass data).

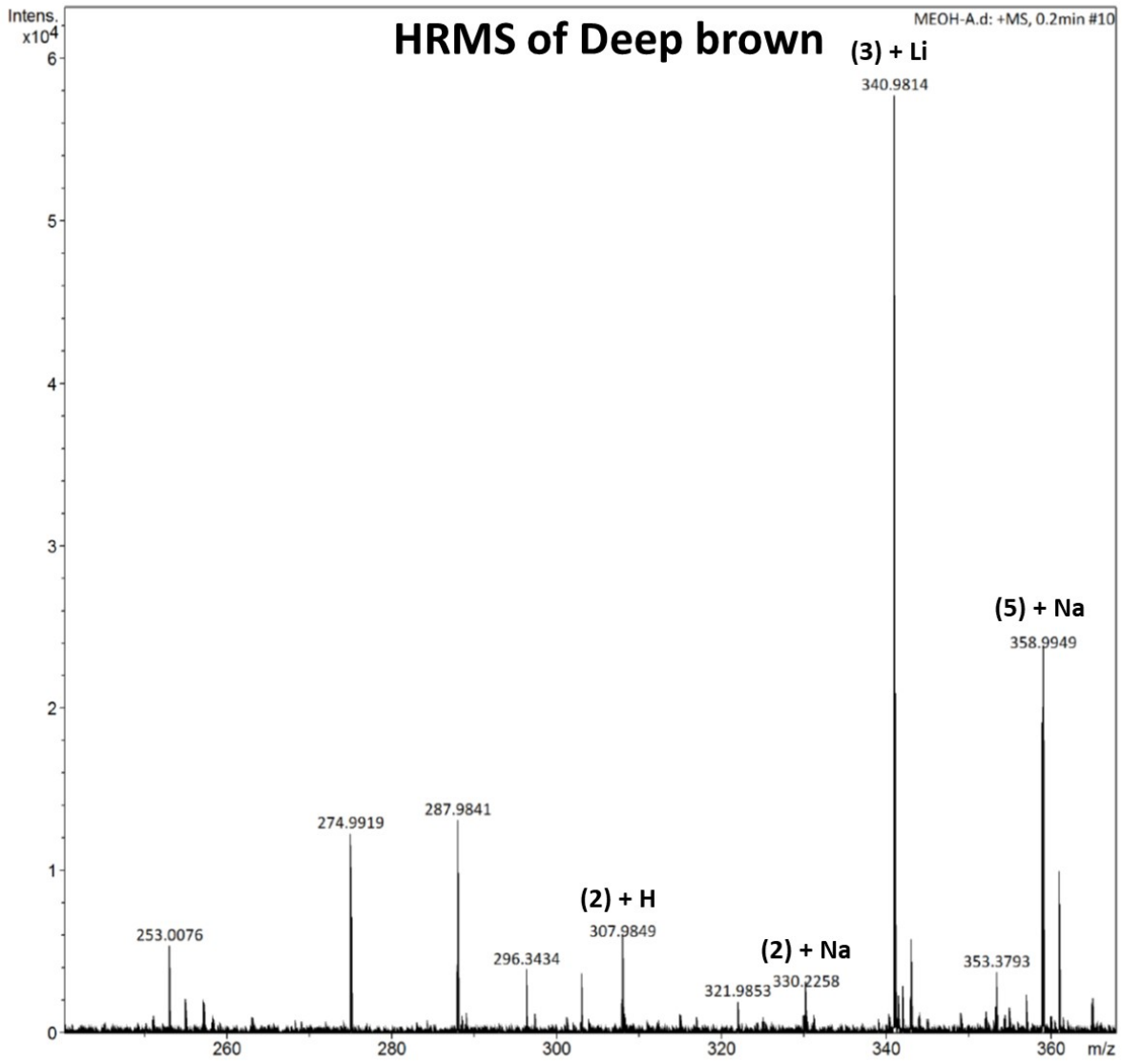

Fig. S12 HRMS spectra of deep brown component.

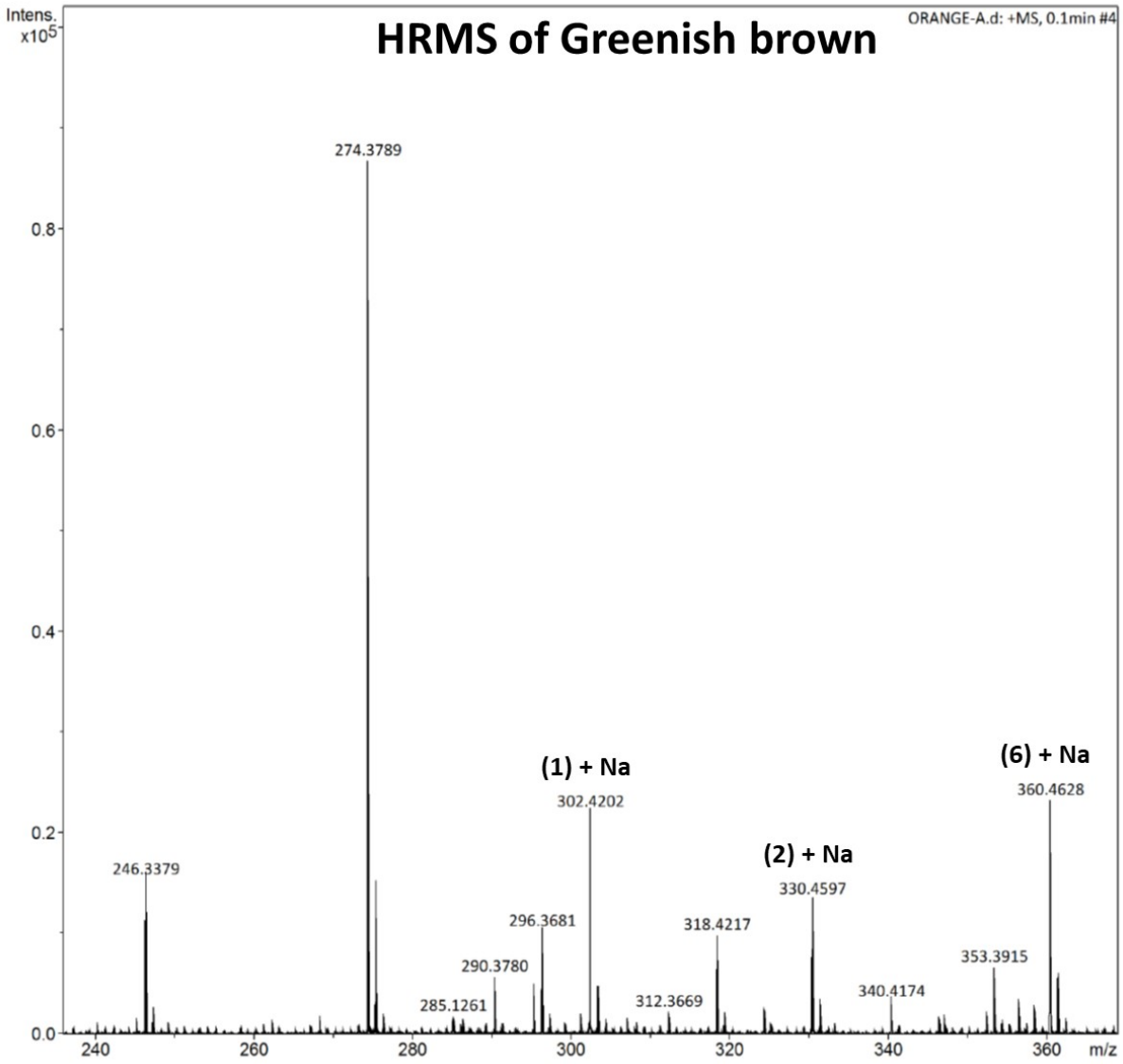

Fig. S13 HRMS spectra of greenish brown component.

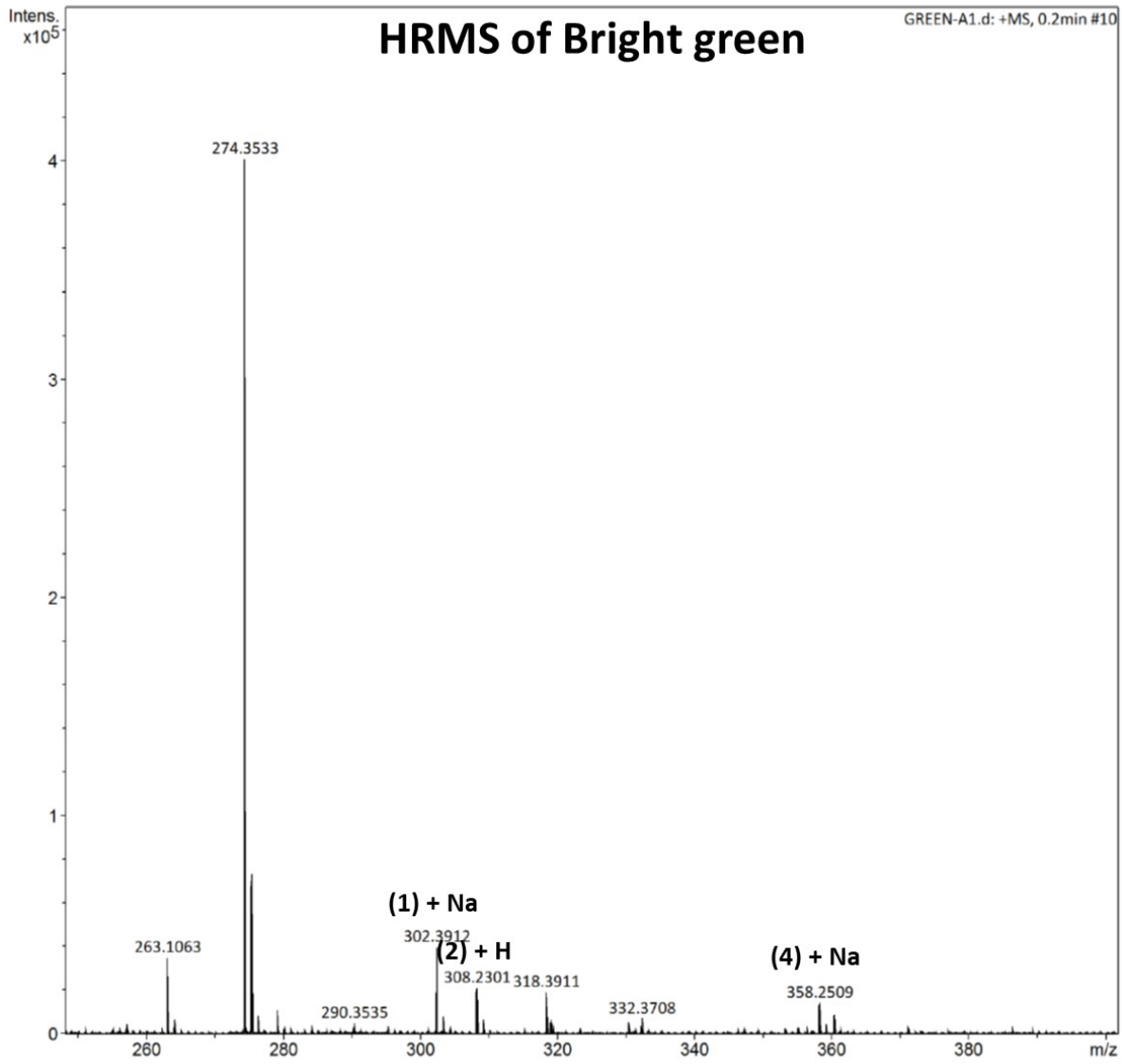

Fig. S14 HRMS spectra of bright green.

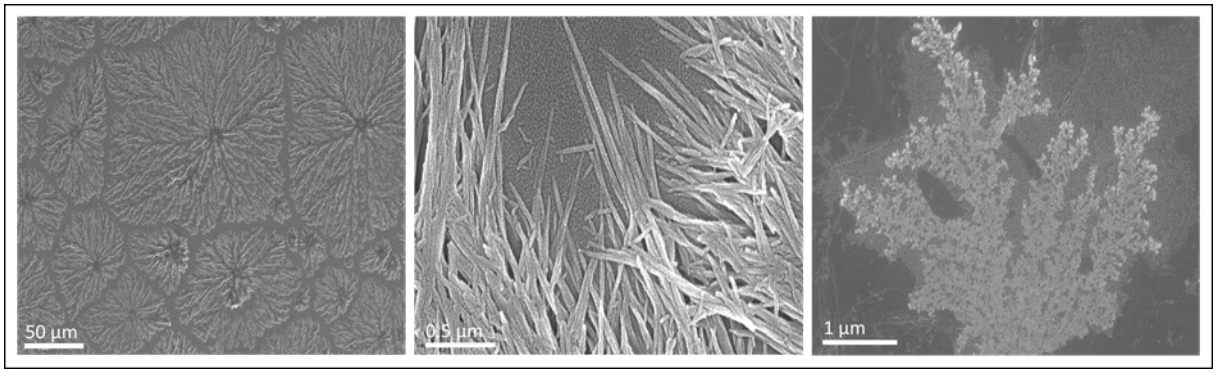

Fig. S15 SEM images of the bright green component under different experimental conditions. Different morphologies appeared due to concentration dependent drying mediated process during sample preparation.

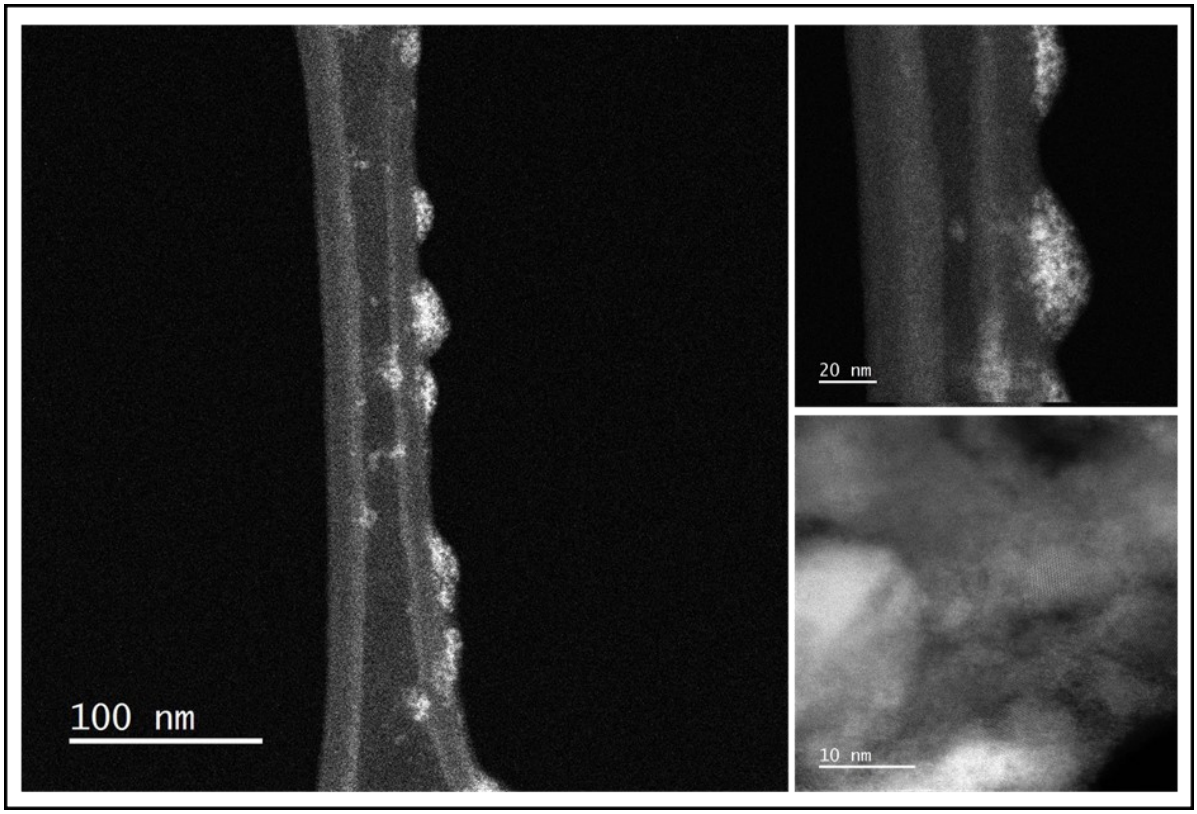

Fig. S16 STEM images of greenish brown component. Free vertically hanging organic chromophores are clearly visible on the side of the lacey carbon grid.

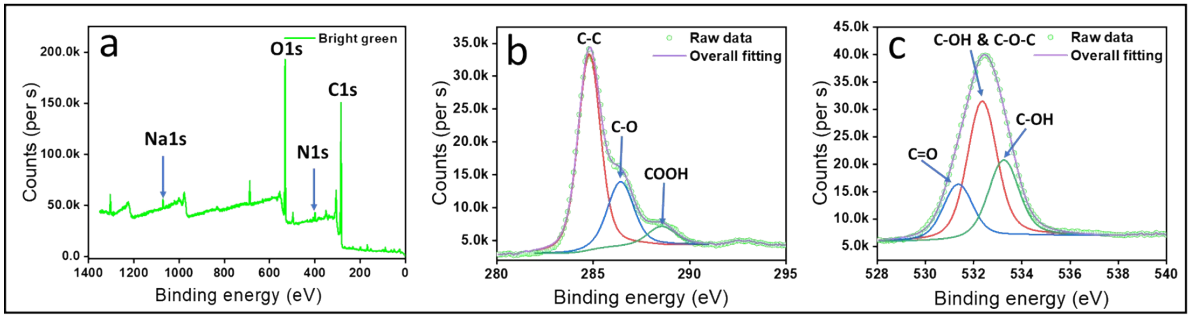

Fig. S17 (a) XPS spectra of bright green component, showing the presence of C1s, O1s and N1s related functional groups. (b-c) High-resolution XPS spectra of C1s where peaks at 284.80, 286.42 and 288.55 eV representing the C-C, C-O and COOH functional groups respectively. (c) High-resolution XPS spectra of O1s where peaks at 531.35 and 532.35 eV representing the C=O, C-OH & C-O-C functional groups.

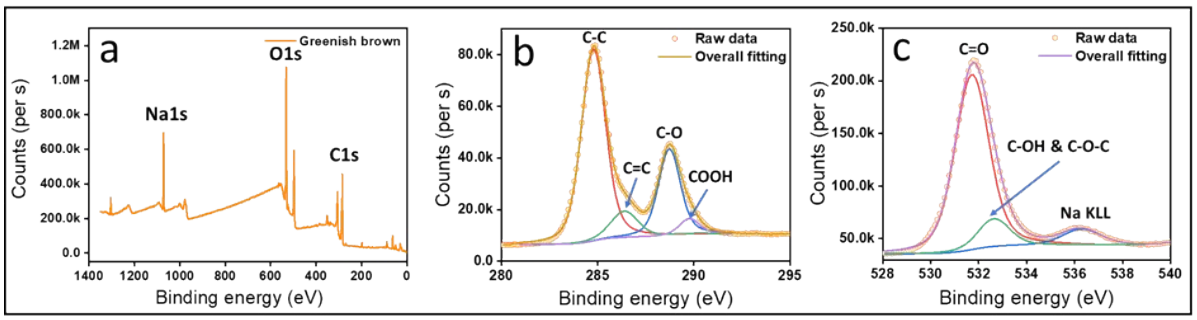

Fig. S18 (a) XPS spectra of greenish brown component. (b-c) High-resolution XPS spectra of C1s where peaks at 284.79, 286.39, 288.73 and 289.77 eV representing the C-C, C=C, C-O and COOH functional groups respectively. (c) High-resolution XPS spectra of O1s where peaks at 531.72 and 532.63 eV representing the C=O, C-OH & C-O-C functional groups.

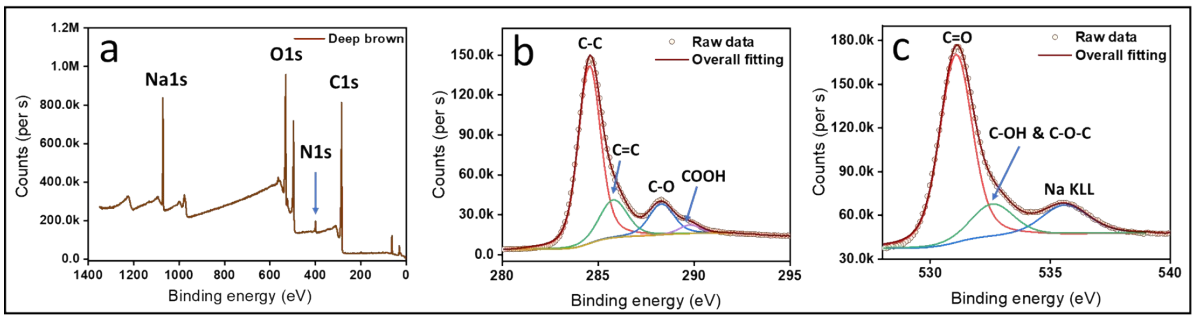

Fig. S19 (a) XPS spectra of deep brown component. (b-c) High-resolution XPS spectra of C1s where peaks at 284.54, 285.79, 288.29 and 289.77 eV representing the C-C, C=C, C-O and COOH functional groups respectively. (c) High-resolution XPS spectra of O1s where peaks at 531.07 and 532.59 eV representing the C=O, C-OH & C-O-C functional groups.

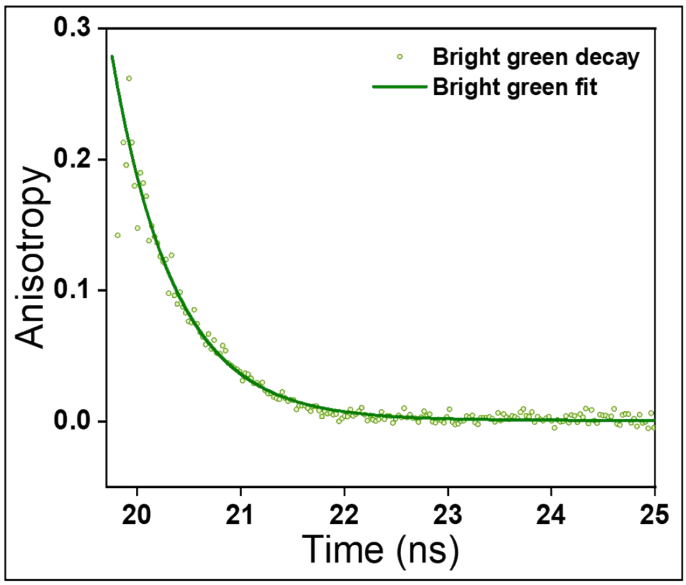

Fig. S20 Fluorescence anisotropy decay of bright green component.

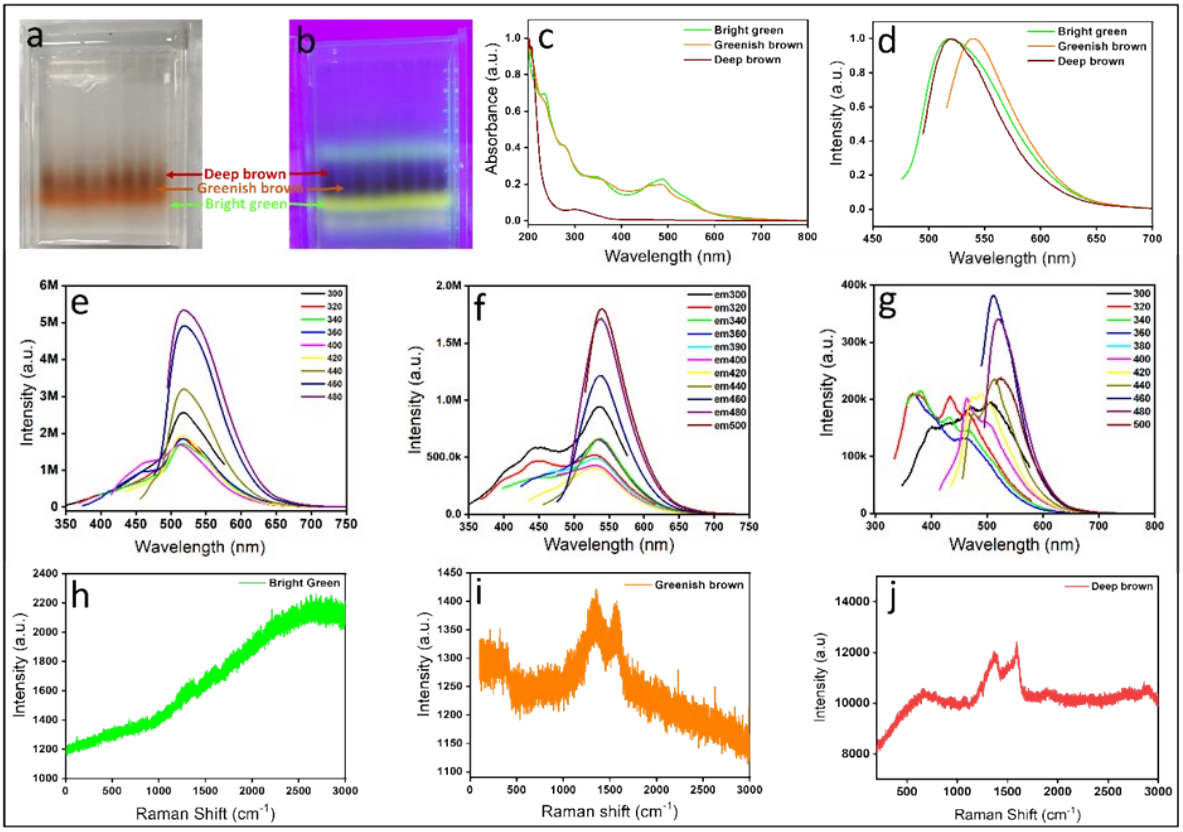

Fig. S21 Agarose gel electrophoresis separation of the synthesized CNDs. Three distinct colors both (a) in naked eye and (b) UV light illumination were observed. (c) Comparative absorption spectra of all three components. (d) Relative normalized steady-state emission spectra of all three separated components. (e-g) excitation wavelength dependent emission spectra of bright green, greenish brown and deep brown components. (h) Raman spectrum of the bright green component with fluorescence background. (i) Raman spectrum of the greenish brown component having D and G bands. (j) Raman spectrum of the deep brown component having D and G bands.

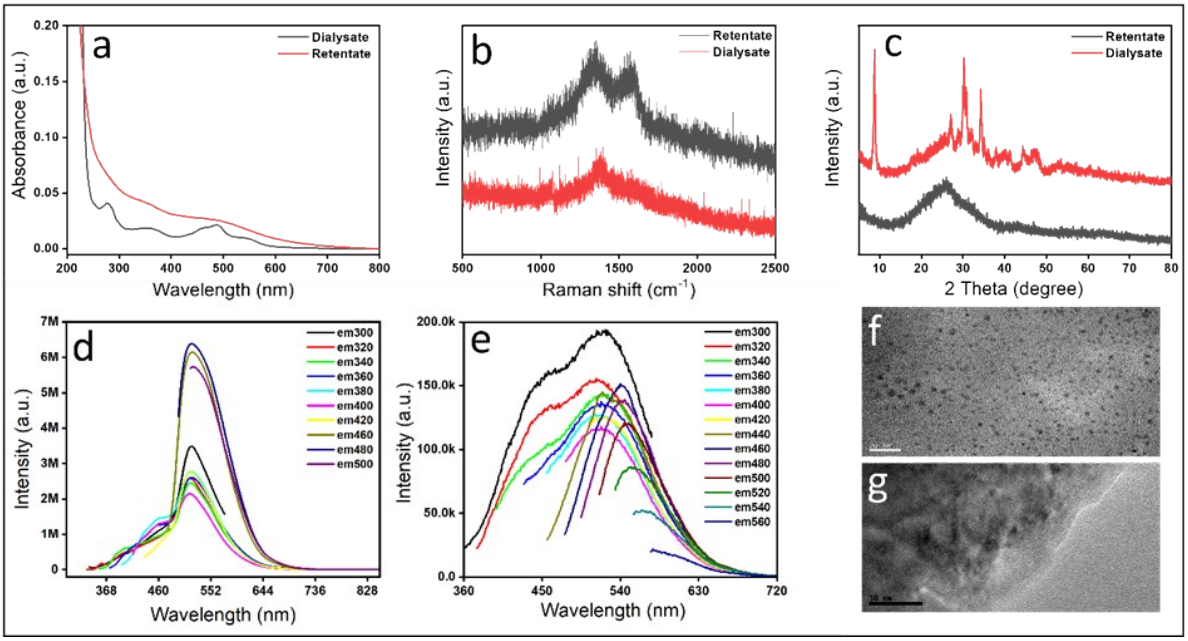

Fig. S22 (a) Absorption spectra of dialysate and retentate obtained after dialysis of crude CNDs. Dialysate showed extensive molecular state emission, while retentate showed major core and edge state with a broad molecular state emission. (b) Raman spectra of dialysate and retentate. Retentate showed D and G bands but dialysate showed no D and G bands. (c) PXRD spectra of retentate and dialysate. Retentate showed broad peak, while dialysate showed structured emission with little broad peak. (d-e) Emission spectra of both dialysate and retentate excited by different wavelength. Dialysate showed excitation independent emission spectra, while retentate showed excitation dependent emission spectra. (f-g) TEM image of retentate and dialysate respectively. The retentate showed the CNDs formation with a size of ~4 nm, while the dialysate showed only aggregated structure.

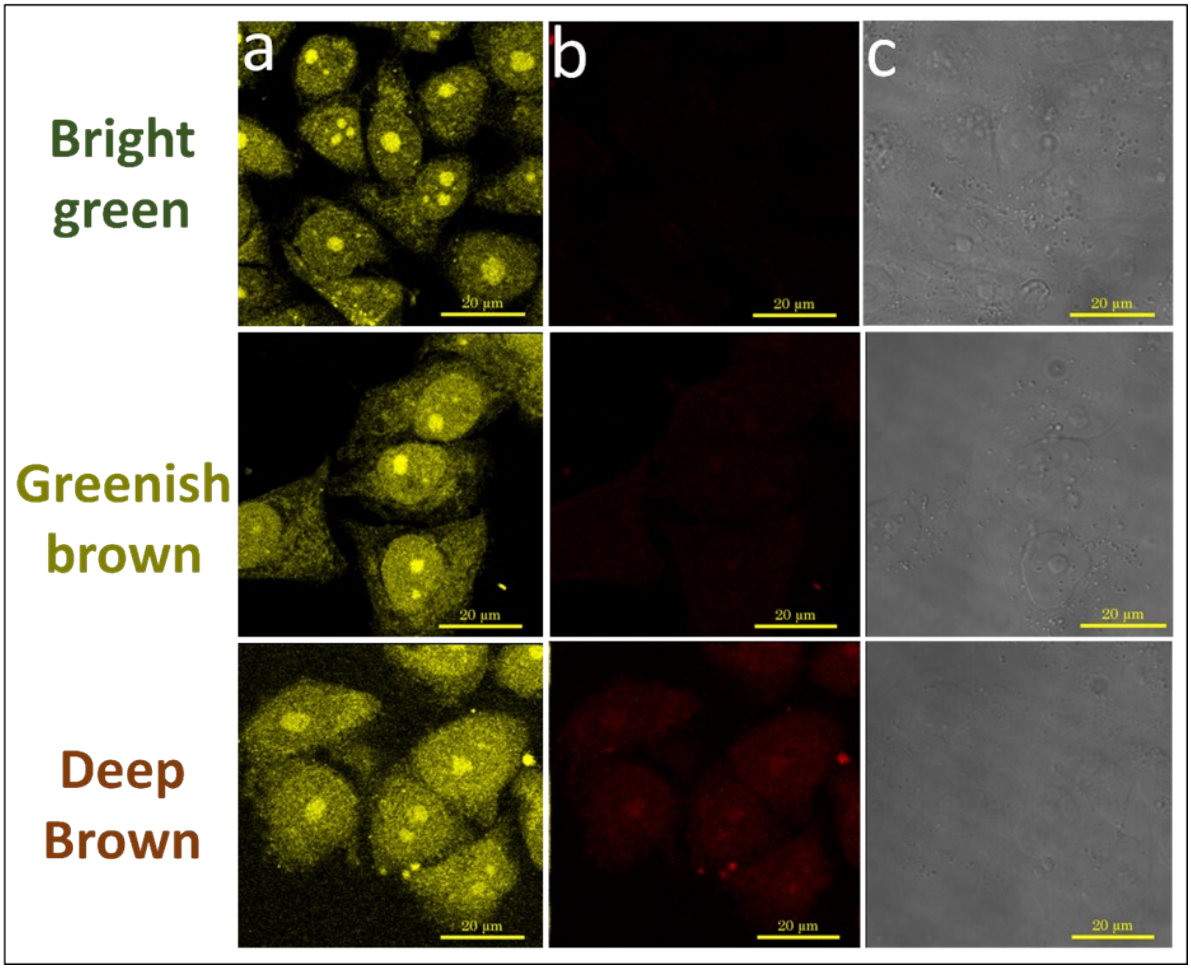

Fig. S23 (a-b) Confocal microscopy images of HeLa cells stained with bright green, greenish brown and deep brown components under different excitation laser wavelengths 488 and 639 nm. The images show that all the components have the high capability to stain the HeLa cell. Little red emission image of the cells was observed for the deep brown component. (c) TD images of the HeLa cells.

Moiety	Binding energy (eV)		Atomic %	
	Greenish brown	Deep brown	Greenish brown	Deep brown
C-C	284.79	284.54	61.0	66.37
C=C	286.39	285.79	9.46	17.67
C-O	288.73	288.29	24.99	12.92
COOH	289.77	289.77	3.94	3.03

Table S1. Deconvoluted C1s spectra showing an increment in the atomic percentage of C=C for deep brown component.